A Simple Carrier-Based Implementation for a General 3-level Inverter Using Nearest Three Space Vector PWM Approach

Aditya Dholakia
Electrical Engineering Department
Indian Institute of Science
Bengaluru, India
adityajd@iisc.ac.in

Sayan Paul
Electrical Engineering Department
Indian Institute of Science
Bengaluru, India
sayanp@iisc.ac.in

Shailesh Ghotgalkar
Texas Instruments
Bengaluru, India
shailgg@ti.com

Kaushik Basu
Electrical Engineering Department
Indian Institute of Science
Bengaluru, India
kbasu@iisc.ac.in

***Abstract*—This paper proposes a novel carrier-based implementation strategy of a standard space-vector pulse-width modulation (SVPWM) technique of three-phase (3ϕ) three-level inverter (TLI). To synthesize the reference voltage vector, the selected SVPWM technique uses nearest three voltage space-vectors in order to reduce output voltage THD and partially balance the neutral point voltage. The implementation complexity of this SVPWM technique is reduced by introducing the concept of common-mode signal in duty-ratio calculation of 3ϕ-TLI. Following the modulation strategy of the selected SVPWM technique, general expression of common-mode signal has been derived in terms of maximum, middle and minimum values of input 3ϕ modulation signals. It is shown in the paper that six duty ratios of 3ϕ-TLI can be directly calculated from the input 3ϕ modulation signals and the derived common-mode signal. Thus, calculation-intensive steps of SVPWM technique, like, identification of reference voltage vector location, calculation of dwell-times of individual vectors, are avoided. The proposed algorithm is validated through simulation in MATLAB and experiment on 1.5 kW hardware prototype.**

***Index Terms*—Three level inverter, Space-vector modulation, Nearest three space-vector PWM, Neutral-point clamped, Common-mode, Carrier comparison**

I. Introduction

Multi-level converter topologies are gaining special attention in medium-voltage high-power applications since last few decades for its' advantages, like, reduced voltage stress, lower harmonic distortion in output voltage, compared to two-level converter, [1], [2]. Three-level inverter (TLI) is one of the most common multi-level inverter and is available in two different configurations: neutral-point clamped (NPC) and T-type. Different space-vector based pulse-width modulation techniques (SVPWM) techniques of TLI are available in the literature where output voltage THD reduction, common-mode voltage reduction, neutral-point voltage balancing are the prime focus, [2], [3].

There are few applications where two independent rectifiers act as two isolated input DC sources for TLI, [4], or, the front-end circuit, such as back-to-back topology or three-level boost circuit, is there to control the voltages across the two DC-link capacitors, [3]. In this case, TLI doesn't suffer from neutral-point voltage balancing problem in these applications. Therefore, popular Nearest Three Space-vectors PWM (NTSVPWM) strategy, as proposed by [5]–[7], can be adopted in these applications to generate output voltages with lower THD.

As TLI has two states with same voltage space-vector, NTSVPWM can be implemented in multiple ways by dividing the duty ratio of the space-vector in different ratios between these two redundant states. This impacts the neutral-point voltage balancing as the redundant states have opposite effects on the neutral-point voltage. The proposed technique of [5], which divides the duty ratio of a space-vector equally between the redundant states, has been considered in this paper for carrier based implementation and calculation complexity reduction. This technique is termed as Conventional NTSVPWM (CNTSVPWM) in this paper. CNTSVPWM balances the neutral-point voltage partially.

Although SVPWM is widely used modulation technique of both two-level and TLI converters, it is calculation-intensive as it involves following steps, as proposed by [7]:

1) Determination of location of reference voltage vector i.e. Sector Identification;
2) Calculation of dwell times of the nearest vectors;
3) Calculation of duty ratios of all the switches based on the applied switching states.

The implementation algorithm of well-known Conventional Space Vector PWM (CSVPWM) technique of two-level inverter has been simplified by introducing the concept of

978-1-7281-5826-6/20/$31.00 ©2020 IEEE

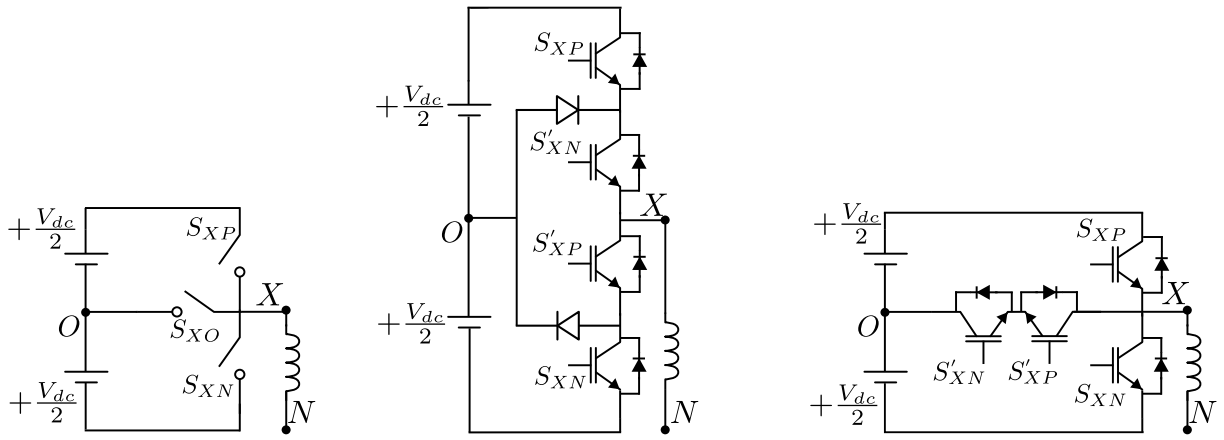

(a) General 3 level (b) NPC-Type (c) T-Type

Figure 1: One leg of 3ϕ-TLI

common-mode or zero-sequence signal. CSVPWM technique can be implemented in carrier comparison way by adding the common-mode voltage to the respective modulating signals of each phase. Similar approach has been taken in this paper to simplify the implementation complexity of popular CNTSVPWM by introducing the concept of common-mode signal. The common-mode signal of CNTSVPWM technique has been generalised in terms of maximum, middle and minimum values of the three modulation signals of three-phase (3ϕ) TLI irrespective of the location of reference voltage vector. Thereafter, the duty ratios of all the switches of 3ϕ-TLI are calculated with the help of this common-mode signal and 3ϕ modulation signals. Thus CNTSVPWM technique is implemented in carrier comparison way after avoiding the aforementioned three steps.

The organization of the paper is as follows. Section II briefly describes the modulation strategy of CNTSVPWM, section III discusses the proposed implementation algorithm by introducing the concept of common-mode. Simulation and experimental validation of the proposed implementation strategy are discussed in section IV; section V concludes this paper.

II. A BRIEF DISCUSSION ON THE MODULATION STRATEGY OF CNTSVPWM

A. Modeling of 3ϕ 3-level inverter

Fig. 1a shows the general structure of one leg of a three-phase (3ϕ) three-level inverter (TLI), where $X \in \{A, B, C\}$. Each leg of TLI has three switches, .viz, S_{XP}, S_{XO} and S_{XN}. To avoid the shorting of the input DC sources, only one of the three switches can be turned 'on' at any given instant of time. To provide continuous path for current flow from the output inductive port, at-least one of these three switches should remain 'on' at any given instant of time. Therefore, one and only one of the three switches should remain 'on' at any given instant of time. Based on this fact, each leg of TLI has three allowable switching states which are denoted by three letters: S_{XP} is 'on' (denoted by P), S_{XO} is 'on' (O) and S_{XN} is 'on' (N). The pole voltage, v_{XO}, in these states is $+\frac{V_{dc}}{2}$, 0 and $-\frac{V_{dc}}{2}$, respectively. As 3ϕ inverter has 3 legs, 3^3 = 27 permissible switching states are there in 3ϕ-TLI. Each of these states are denoted by three ordered letters, xyz, where x, y and z represent the switching states of the legs A, B and C, respectively, and $x, y, z \in \{P, O, N\}$. Therefore, switching state PON implies S_{AP}, S_{BO} and S_{CN} are on and therefore, $v_{AO} = +\frac{V_{dc}}{2}$, $v_{BO} = 0$ and $v_{CO} = -\frac{V_{dc}}{2}$.

Each leg of TLI in Fig. 1a can be realized either by neutral-point clamped (NPC) or T-Type configurations, as shown in Fig. 1b and 1c, respectively, where, switch pairs (S_{XP}, S'_{XP}) and (S_{XN}, S'_{XN}) operate in complementary fashion. S_{XO} is implemented using S'_{XP} and S'_{XN} in Fig. 1b and 1c.

$$\begin{aligned} v_\alpha + jv_\beta &= \frac{2}{3}(v_{AN} + v_{BN}e^{j\frac{2\pi}{3}} + v_{CN}e^{-j\frac{2\pi}{3}}) \\ &= \frac{2}{3}(v_{AO} + v_{BO}e^{j\frac{2\pi}{3}} + v_{CO}e^{-j\frac{2\pi}{3}}) \end{aligned} \tag{1}$$

To model a 3ϕ balanced load with an isolated neutral point, standard 3ϕ-2ϕ Clarke's transformation is applied on three line-neutral voltages, v_{XN}, or pole voltages, v_{XO}, as shown in (1). Both of these result into same space-vector in $\alpha - \beta$ plane. With this transformation, all 27 switching states of 3ϕ-TLI can be mapped into $\alpha - \beta$ plane. For example, plugging the pole voltages generated by switching state PON in (1), following space-vector is obtained.

$$(v_\alpha + jv_\beta)|_{PON} = \frac{V_{dc}}{\sqrt{3}}e^{j\frac{\pi}{6}}$$

Fig. 2a shows the mapping of 27 states in $\alpha-\beta$ plane where the lengths of the vectors are scaled with the factor $\frac{1}{V_{dc}}$. The resultant hexagonal structure can be divided into six equivalent sectors, as shown in Fig. 2a.

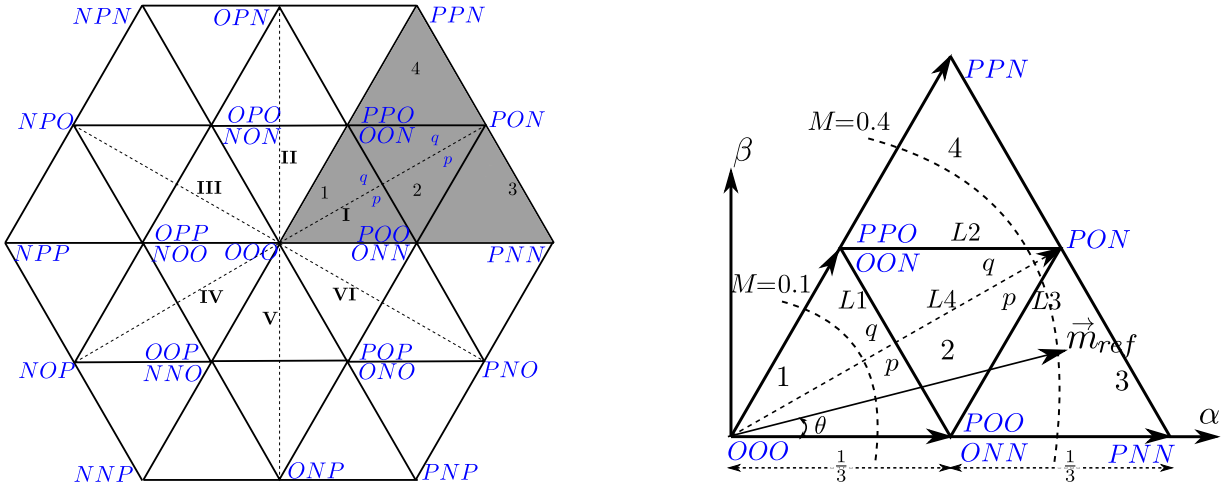

(a) Mapping of 27 switching states in $\alpha - \beta$ plane

(b) Sector-I

Figure 2: Voltage space-vectors and reference voltage vector in $\alpha - \beta$ plane

When the transformation of (1) is applied on the average line-neutral voltages, $\overline{v}_{XN}$ where $X \in \{A, B, C\}$, reference voltage vector, $\vec{V}_{ref}$, is obtained, as given in (2a). To fit this reference voltage vector in Fig. 2a, all the variables are scaled by a factor of $\frac{1}{V_{dc}}$, which gives (2b). Here, $\vec{m}_{ref} = \frac{\vec{V}_{ref}}{V_{dc}}$, $m_X = \frac{\overline{v}_{XN}}{V_{dc}}$, $\sum_X m_X = 0$ for balanced 3ϕ load with isolated neutral point.

$$\vec{V}_{ref} = \frac{2}{3}(\overline{v}_{AN} + \overline{v}_{BN}e^{j\frac{2\pi}{3}} + \overline{v}_{CN}e^{-j\frac{2\pi}{3}}) \tag{2a}$$

$$\vec{m}_{ref} = \frac{2}{3}(m_A + m_B e^{j\frac{2\pi}{3}} + m_C e^{-j\frac{2\pi}{3}}) \tag{2b}$$

B. Modulation Strategy

Based on the values of $m_{A,B,C}$, tip of $\vec{m}_{ref}$ can lie in any of the six equivalent sectors. This paper discusses the modulation strategy w.r.t. sector-I and the zoomed version of sector-I is shown in Fig. 2b. To realize $\vec{m}_{ref}$, Conventional Nearest Three Space-Vector PWM (CNTSVPWM) technique is used to minimize the ripple voltage. According to this technique, sector-I is divided into 4 subsectors (SS) and each of subsector-1 (SS-1) and subsector-2 (SS-2) is further subdivided into p and q regions, as shown in Fig. 2b.

Table I lists the seven-segment switching sequences within a sampling period, T_s, as proposed by [7], in different sub-sectors and sub-subsectors of sector-I. In $\{1p, 2p\}$ and $\{1q, 2q\}$, switching states $\{POO, ONN\}$ and $\{PPO, OON\}$, respectively, are applied for equal amount of time within T_s. An important observation one should make here is that none of the three legs of 3ϕ-TLI apply both P and N states within one T_s. Therefore, CNTSVPWM technique results in unipolar modulation.

Let the nearest three voltage space-vectors of $\vec{m}_{ref}$ be $\vec{V}_1, \vec{V}_2$ and $\vec{V}_3$ and duty ratios of application of these vectors be d_1, d_2 and d_3. These duty ratios can be determined in terms of m_A, m_B and m_C by solving the system of equations given in (3).

Table I: Switching sequences in different subsectors (SS) of sector-1

Subsector	Switching Sequence
1p	*ONN-OON-OOO-POO-OOO-OON-ONN*
1q	*OON-OOO-POO-PPO-POO-OOO-OON*
2p	*ONN-OON-PON-POO-PON-OON-ONN*
2q	*OON-PON-POO-PPO-POO-PON-OON*
3	*ONN-PNN-PON-POO-PON-PNN-ONN*
4	*OON-PON-PPN-PPO-PPN-PON-OON*

$$\begin{aligned}\vec{m}_{ref} &= d_1\vec{V}_1 + d_2\vec{V}_2 + d_3\vec{V}_3 \\ &= \frac{2}{3}(m_A + m_B e^{j\frac{2\pi}{3}} + m_C e^{j\frac{-2\pi}{3}})\end{aligned} \tag{3a}$$

$$d_1 + d_2 + d_3 = 1 \tag{3b}$$

Based on the status of the three switches of each leg in the applied switching states, duty values of all three switches corresponding to each leg, d_{XP}, d_{XO} and d_{XN}, can be determined. For example, when tip of $\vec{m}_{ref}$ lies within subsector-3, $\vec{V}_1 = \vec{V}_{ONN/POO} = \frac{1}{3}$, $\vec{V}_2 = \vec{V}_{PNN} = \frac{2}{3}$ and $\vec{V}_3 = \vec{V}_{PON} = \frac{1}{\sqrt{3}}e^{j\frac{\pi}{6}}$. d_1, d_2 and d_3 can be expressed in terms of m_A, m_B and m_C as shown below.

$$\begin{aligned}d_1 &= 2 - 2(m_A - m_C); \\ d_2 &= 2(m_A - m_B) - 1; \\ d_3 &= 2(m_B - m_C).\end{aligned}$$

Switch S_{AP} is 'on' when states POO, PNN and PON are applied and therefore, $d_{AP} = \frac{d_1}{2} + d_2 + d_3$ as POO is

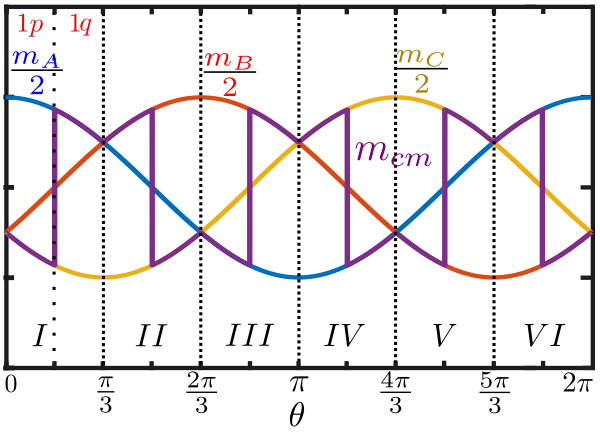

Figure 3: M = 0.1

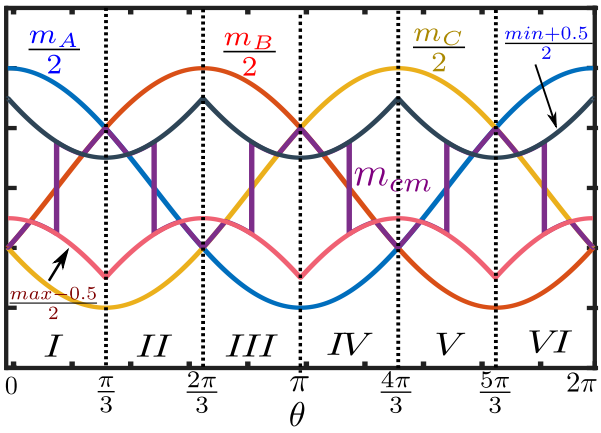

Figure 4: M = 0.4

applied for $\frac{d_1}{2}$. Similarly, duty ratios of other switches can be calculated for subsector-3. Plugging the values of d_1, d_2 and d_3, the duty ratios of all the switches corresponding to subsector-3 are given here in terms of m_A, m_B and m_C:

$$d_{AP} = m_A - m_C;$$
$$d_{BN} = -3m_B;$$
$$d_{CN} = m_A - m_C;$$
$$d_{AN} = d_{BP} = d_{CP} = 0;$$
$$d_{XO} = 1 - d_{XP} - d_{XN};\ where\ X \in \{A, B, C\}$$

One can verify from above duty ratio expressions that the discussed modulation strategy results into unipolar PWM scheme. Similar to the above example, duty ratios of all the switches of three legs can be determined in terms of m_A, m_B and m_C for subsectors of other sectors as well.

III. Proposed Implementation Strategy of CNTSVPWM

A. Determination of Common-mode Signal

As the pole voltage, v_{XO}, generated by switches S_{XP}, S_{XO} and S_{XN} in Fig. 1a are $+\frac{V_{dc}}{2}$, 0 and $-\frac{V_{dc}}{2}$, respectively, average pole voltage is $\overline{v}_{XO} = (d_{XP} - d_{XN})\frac{V_{dc}}{2}$. Applying KVL on loop OXN of Fig. 1a, we get $\overline{v}_{XO} = \overline{v}_{XN} + \overline{v}_{NO}$. Comparing these two equations in (4), common-mode signal, m_{cm} can be determined, where $m_{cm} \triangleq \frac{\overline{v}_{NO}}{V_{dc}}$.

$$\overline{v}_{XO} = (d_{XP} - d_{XN})\frac{V_{dc}}{2} = \overline{v}_{XN} + \overline{v}_{NO} \tag{4a}$$

$$m_{cm} \triangleq \frac{\overline{v}_{NO}}{V_{dc}} = \frac{1}{2}(d_{XP} - d_{XN}) - m_X \tag{4b}$$

Substituting d_{XP}, d_{XN} for any X, as already obtained in section II-B, one can determine m_{cm} in terms of m_A, m_B and m_C.

For example, m_{cm} in subsector-3 can be calculated from the six duty cycles and (4). For leg A, $d_{AP} = m_A - m_C$ and $d_{AN} = 0$. Plugging these values of d_{AP} and d_{AN} in (4b), while keeping in mind $m_A + m_B + m_C = 0$, the obtained value of common mode, m_{cm}, is $\frac{m_B}{2}$. Here, the leg A has been considered for calculating m_{cm}, but, in general, any leg can be used to calculate m_{cm} which will result in the same value of m_{cm}. Similarly, m_{cm} for other subsectors and sub-subsectors of sector-I are calculated and listed in Table II.

When m_{cm} of subsectors and sub-subsectors of other sectors were evaluated, it was seen that m_{cm} signal can be generalised in terms of max, min and mid signals irrespective of the sector where tip of $\vec{m}_{ref}$ lies. Here, max=maximum$\{m_A, m_B, m_C\}$; min=minimum$\{m_A, m_B, m_C\}$; mid=middle$\{m_A, m_B, m_C\}$. This generalised m_{cm} is tabulated in Table II.

Fig. 3 plots m_{cm} signal along with sinusoidal $\frac{m_A}{2}$, $\frac{m_B}{2}$ and $\frac{m_C}{2}$, where $m_A = M\cos\theta$, $m_B = M\cos(\theta - \frac{2\pi}{3})$, $m_C = M\cos(\theta - \frac{4\pi}{3})$ with $M = 0.1$. For this small value of M, tip of $\vec{m}_{ref}$ lies within subsector-1 throughout all the sectors, as shown in Fig. 2b. M in Fig. 4 is 0.4 and the tip of $\vec{m}_{ref}$ cuts subsectors 2, 3 and 4 for all the sectors. Fig. 4 plots m_{cm}, $\frac{m_A}{2}$, $\frac{m_B}{2}$, $\frac{m_C}{2}$, $\frac{max - 0.5}{2}$ and $\frac{min + 0.5}{2}$.

Table II: Common Mode for each subsector

Subsector	Sector 1	Generalized
1p	$\frac{m_C}{2}$	$\frac{min}{2}$
1q	$\frac{m_A}{2}$	$\frac{max}{2}$
2p	$\frac{m_A - 0.5}{2}$	$\frac{max - 0.5}{2}$
2q	$\frac{m_C + 0.5}{2}$	$\frac{min + 0.5}{2}$
3	$\frac{m_B}{2}$	$\frac{mid}{2}$
4	$\frac{m_B}{2}$	$\frac{mid}{2}$

Table III: Equations (Eq.) of $L1 - L4$

Lines	Eq. in sector-I	Eq. in generalised sector
L1	$m_A - m_C = \frac{1}{2}$	$max - min = \frac{1}{2}$
L2	$m_B - m_C = \frac{1}{2}$	$mid - min = \frac{1}{2}$
L3	$m_A - m_B = \frac{1}{2}$	$max - mid = \frac{1}{2}$
L4	$m_B = 0$	$mid = 0$

Table IV: Subsector and Sub-subsector Identification

if/else	Condition	Subsector/Sub-subsector
if	$max - min \leq \frac{1}{2}$	1
else if	$max - mid \geq \frac{1}{2}$	3
else if	$mid - min \geq \frac{1}{2}$	4
else	-	2
if	$mid \leq 0$	p
else	-	q

B. Identification of Subsector and Sub-subsector

The subsector (SS) and sub-subsector (SSS) within the sector-I can be identified by checking the tip of $\vec{m}_{ref}$ lies on which side of four lines, $L1$, $L2$, $L3$ and $L4$, as shown in Fig. 2b. Suppose, the real and imaginary parts of $\vec{m}_{ref}$ are denoted by α and β, respectively, i.e., $Re\{\vec{m}_{ref}\} = \alpha$ and $Im\{\vec{m}_{ref}\} = \beta$. As $\vec{m}_{ref} = \frac{2}{3}(m_A + m_B e^{j\frac{2\pi}{3}} + m_C e^{-j\frac{2\pi}{3}})$, as given in (2b), α, β are as follows.

$$\alpha = \frac{2}{3}(m_A - \frac{m_B}{2} - \frac{m_C}{2}); \quad \beta = \frac{1}{\sqrt{3}}(m_B - m_C) \qquad (5)$$

Equations of all four lines, $L1$, $L2$, $L3$ and $L4$, can be written in terms of α and β. For example, equation of $L1$, passing through the point $(\frac{1}{3}, 0)$ with a slope of $\tan 120°$, is

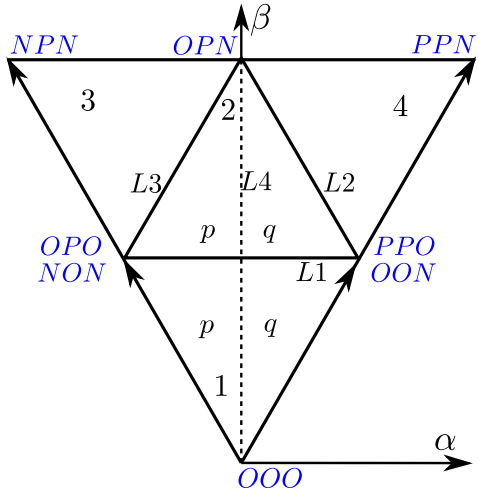

Figure 5: Sector-II

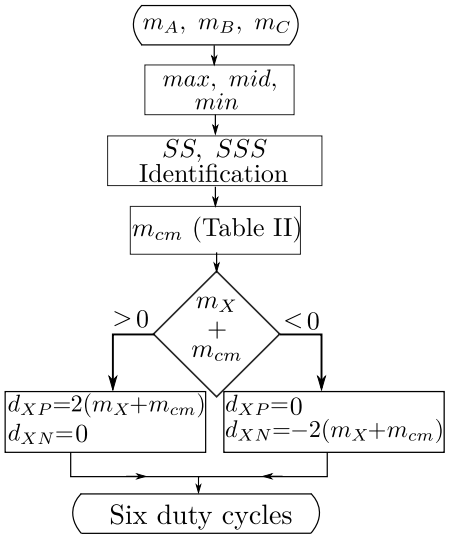

Figure 6: Flow Chart

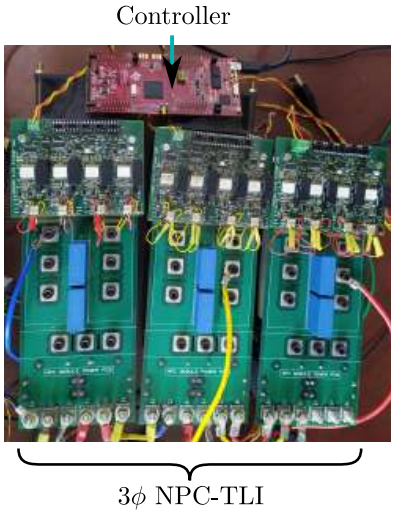

Figure 7: Hardware set-up

$\sqrt{3}\alpha + \beta = \frac{1}{\sqrt{3}}$. Substituting α, β from (5), $m_A - m_C = \frac{1}{2}$ is the condition obtained when (α, β) is on $L1$. Similarly, conditions for tip of $\vec{m}_{ref}$ to lie on lines $L1 - L4$ in terms of m_A, m_B and m_C are tabulated in Table III.

When the equations of these lines are determined in other sectors, it has been observed that these equations can be generalised in terms of max, min and mid and these relationships are furnished in Table III. With these expressions, the conditions given in Table IV should be checked in the given order to identify the subsectors and sub-subsectors.

It is important to mention here that positions of different subsectors and sub-subsectors within a sector are different for odd and even sectors. For example, Fig. 5 shows the different subsectors and sub-subsectors within sector-II. One can easily identify that Fig. 5 is not the same as $60°$ rotated

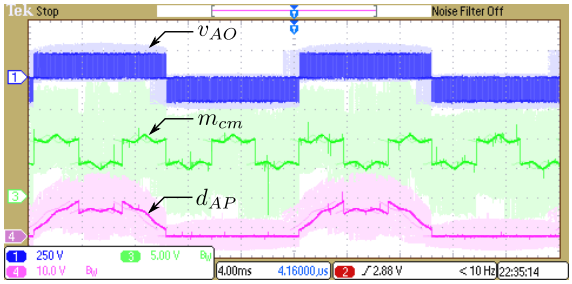

Voltage Scale (V/div): v_{AO}: 250 ; m_{cm}:5 ; d_{AP}:10

(a) Experimental v_{AO}, m_{cm}, d_{AP}

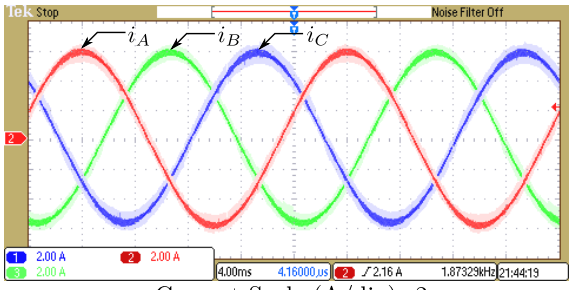

Current Scale (A/div): 2

(b) Experimental 3ϕ load currents

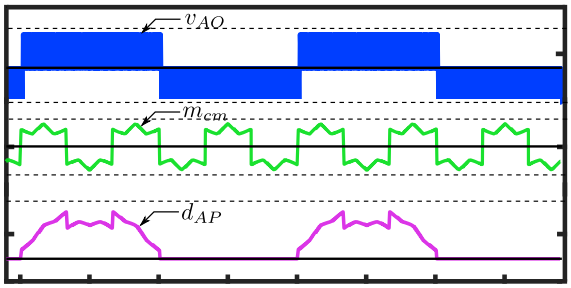

Voltage Scale (V/div): v_{AO}: 250 ; m_{cm}:5 ; d_{AP}:10

(c) Simulated v_{AO}, m_{cm}, d_{AP}

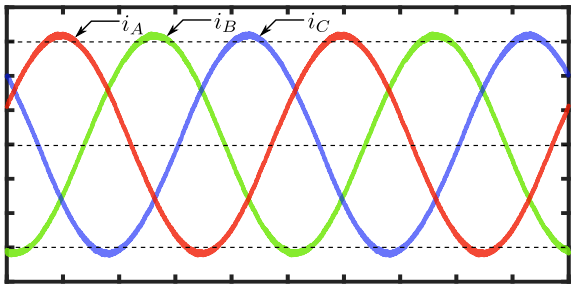

Current Scale (A/div): 2

(d) Simulated 3ϕ load currents

Figure 8: Experimental and simulated waveforms of proposed algorithm at $M = 0.4$; Time Scale = 4 ms/div.

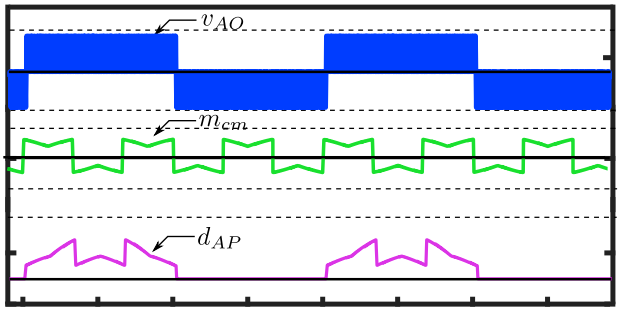

Voltage Scale (V/div): v_{AO}: 250 ; m_{cm}:5 ; d_{AP}: 5

Figure 9: Simulated v_{AO}, m_{cm}, d_{AP} - M = 0.1

version of Fig. 2b w.r.t. positions of the subsectors and sub-subsectors. Positions of SS-3, SS-4 and SSS-p and SSS-q are interchanged. But the boundary lines separating these subsectors and sub-subsectors remain same, i.e., boundary lines between SS-1 and SS-2, SS-2 and SS-4, SS-2 and SS-3, and SSS-p and SSS-q are $L1$, $L2$, $L3$ and $L4$, respectively, and their generalised expressions are same as given in Table III. The labelling of subsectors and sub-subsectors of odd and even sectors will follow those of sector-I and sector-II, respectively.

C. Step by Step Algorithm for Implementation of CNTSVPWM

Following steps are followed by the PWM modulator to determine the six duty ratios, d_{XP} and d_{XN} where $X \in \{A, B, C\}$, from the given modulation signals, m_A, m_B and m_C, which are the output of the controller. The 3ϕ-TLI can be realized either by NPC or T-type configuration. By comparing these duty ratios with triangular carrier, varying from 0 to 1, gating signals of switches S_{XP} and S_{XN} are obtained. The gating pulses of S'_{XP} and S'_{XN} are obtained by complementing the gating signals of S_{XP} and S_{XN}, respectively. This results into seven-segment sequence, as shown in Table I. Fig. 6 shows these steps in flow-chart diagram.

1) From the given m_A, m_B and m_C, find max, mid and min.
2) Identify the subsectors and sub-subsectors based on Table IV. From the subsector and sub-subsector information, determine m_{cm} based on Table II (third column).
3) From (4), we can see that $\frac{\overline{v}_{XO}}{V_{dc}} = \frac{1}{2}(d_{XP} - d_{XN}) = m_X + m_{cm}$. In section-II-B, we saw that CNTSVPWM technique results into unipolar PWM, which means,
   - If $\overline{v}_{XO} > 0$ or $(m_X + m_{cm}) > 0$; $d_{XN} = 0$ and $d_{XP} = 2(m_X + m_{cm})$.
   - If $\overline{v}_{XO} \leq 0$ or $(m_X + m_{cm}) \leq 0$; $d_{XP} = 0$ and $d_{XN} = -2(m_X + m_{cm})$.

   Plugging $X = A, B, C$; all six duty ratios are obtained.

IV. Experimental and Simulation Results

The proposed algorithm is verified through simulation in MATLAB and experiment on a 1.5 kW NPC-TLI prototype. Fig. 7 shows the hardware set-up where 1200 V, 75 A IGBT (SKM75GB123D) and diode (MEE 75-12 DA) modules are used for each leg of 3ϕ NPC-TLI; TMS320F28379D of TI is used as controller card. The operating conditions for both experiment and simulation waveforms of Fig. 8 are as shown in Table V.

Table V: Operating conditions for experiment and simulation

Quantity	Value
Input DC Voltage(V_{dc})	400 V
Modulation Index (M)	0.4
Output frequency (f_{out})	50 Hz
Sampling frequency (f_s)	10 kHz
Load Resistance	25 Ω
Load Inductance	12 mH

Fig. 8b and 8d show the experimental and simulated balanced 3ϕ load currents. The pole voltage of A phase, i.e., v_{AO}, m_{cm} and d_{AP} of experiment and simulation are shown in Fig. 8a and 8c, respectively. The experimental m_{cm} and d_{AP} waveforms are taken through Digital-Analog converter sitting inside the controller board. The unipolar nature of CNTSVPWM technique can be confirmed from v_{AO} waveform; d_{AP} is zero during negative half of v_{AO} or when average A-phase pole-voltage is negative. The calculated value of the peak value of current for M = 0.4 using the values of known parameters turns out to be $6.35A$, also, the value of peak load current observed for same modulation index is approximately $6.15A$. The close agreement of simulation and experimental waveforms with analysis validates the proposed algorithm. Further, simulation results for M = 0.1 have been given in Fig. 9 which can be compared with Fig. 3 for the validation of common mode waveform, m_{cm}.

V. Conclusion

The Nearest Three Space-Vector PWM (NTSVPWM) strategy with equal application of redundant states results in high quality output voltage and partial neutral point balancing and is important where the split DC link is actively controlled. The proposed implementation strategy of Conventional Nearest Three Space-Vector PWM (CNTSVPWM) technique calculates the six duty ratios of three-phase three-level inverter directly from the given input 3ϕ modulation signals and common-mode signal. The expression of common-mode signal has been derived in terms of maximum, middle and minimum values of 3ϕ modulation signals at any given instant. Following this strategy, six duty ratios can be calculated in three steps with very minimal amount of code and computation time.

References

[1] S. Busquets-Monge, J. Bordonau, D. Boroyevich, and S. Somavilla, "The nearest three virtual space vector pwm-a modulation for the comprehensive neutral-point balancing in the three-level npc inverter," *IEEE power electronics letters*, vol. 2, no. 1, pp. 11–15, 2004.

[2] C. Xia, G. Zhang, Y. Yan, X. Gu, T. Shi, and X. He, "Discontinuous space vector pwm strategy of neutral-point-clamped three-level inverters for output current ripple reduction," *IEEE Transactions on Power Electronics*, vol. 32, no. 7, pp. 5109–5121, 2016.

[3] J. Weidong, L. Wang, J. Wang, X. Zhang, and P. Wang, "A carrier-based virtual space vector modulation with active neutral-point voltage control for a neutral-point-clamped three-level inverter," *IEEE Transactions on Industrial Electronics*, vol. 65, no. 11, pp. 8687–8696, 2018.

[4] R. Sommer, A. Mertens, C. Brunotte, and G. Trauth, "Medium voltage drive system with npc three-level inverter using igbts," 2000.

[5] C. Lee, S. Hui, H. Shu-HungChung, and Y. Shrivastava, "A randomized voltage vector switching scheme for three-level power inverters," *IEEE Transactions on Power Electronics*, vol. 17, no. 1, pp. 94–100, 2002.

[6] A. K. Gupta and A. M. Khambadkone, "A space vector pwm scheme for multilevel inverters based on two-level space vector pwm," *IEEE Transactions on industrial electronics*, vol. 53, no. 5, pp. 1631–1639, 2006.

[7] B. Wu and M. Narimani, *High-power converters and AC drives*. John Wiley & Sons, 2017.